16th World Conference on Earthquake, 16WCEE 2017

Santiago Chile, January 9th to 13th 2017

Paper N° 3149 (Abstract ID)

Registration Code: S-V1463171040

Tsunami Risk for Insurance Portfolios from Megathrust Earthquakes in Cascadia Subduction Zone

R. J. Farahani [(1)], J. Woessner [(2)], S. Bingi [(3)], I. Charvet [(4)], Ch. Williams [(5)], M. Nyst [(6)], M. Masuda [(7)], J. Bryngelson [(8)], N. Shome [(9)]

[(1)] Senior Modeler, Risk Management Solutions, USA, rozita.farahani@rms.com
[(2)] *Lead Modeler, Risk Management Solutions, Switzerland, Jochen.Woessner@rms.com*
[(3)] *Manager, Risk Management Solutions, India, Sreenivas.Bingi@rms.com*
[(4)] *Senior Modeler, Risk Management Solutions, UK, Ingrid.charvert@rms.com*
[(5)] *Senior Director, Risk Management Solutions, USA, Chesley.Williams@rms.com*
[(6)] *Director, Risk Management Solutions, USA, Marleen.Nyst@rms.com*
[(7)] *Senior Director, Risk Management Solutions, USA, Manabu.Masuda@rms.com*
[(8)] *Director, Risk Management Solutions, USA, Jason.Bryngelson@rms.com*
[(9)] *Senior Director, Risk Management Solutions, USA, Nilesh.shome@rms.com*

Abstract

The 2011 Tohoku megathrust earthquake of magnitude 9.0 (M_W) showed the potential of significant loss to insurance industry due to tsunami. Large magnitude earthquakes at the Cascadia Subduction Zone (CSZ) can cause the most devastating tsunami hazard in the pacific basin to the west coast of USA including Washington, Oregon, and north California coastlines. The perception of tsunami risk in the industry has been small compared to the risk from the shake damage. To improve managing the tsunami risk for USA coastal cities, Risk management Solution (RMS) first modeled the historical 1700 Cascadia tsunami event and evaluated the maximum tsunami waves at different stations offshore of west coast of USA as well as coastal inundation. Then we developed a set of stochastic slip distributions along the CSZ corresponding to the large earthquakes with moment magnitude (M_W) higher than 8.0 and modeled the tsunami wave propagation and coastal inundation. Each tsunami event is built based on seismic characteristics of the CSZ ruptures and a slip model that provides a non-uniform slip distribution. Non-uniform slip distributions are used to provide a realistic set of possible tsunami generating earthquakes and are constrained by the paleo-seismic records of offshore uplifts along west of USA. The vertical seafloor/coastline deformations including uplift and subsidence are computed using a triangular dislocation model that captures the complexities of the subduction zone geometry. These deformations are then used as initial conditions to a high-resolution numerical model that simulates the tsunami wave propagation and coastal inundations. Parallel computations are applied on Graphic Processing Units (GPUs) to overcome the large numerical computational efforts needed to model the entire west coast of USA. Variable land surface roughness based on land cover data is used to simulate the accurate hydraulics of coastal inundation. The tsunami hazard maps are developed for the entire west coast of USA starting from Washington state coast at north to California state coasts in south. In addition the histograms of maximum tsunami waves for key coastal cities are provided. This paper mainly covers the hazard aspect of tsunami evaluation and simulation for west coast of USA. In parallel RMS has developed an extensive study on the vulnerability of infrastructures and buildings along west of USA as well as the detailed information of exposure. The hazard model will later be combined with the vulnerability model and exposure model to provide a comprehensive understanding of tsunami risk and economic loss along the west coast of USA due to megathrust earthquakes in CSZ.

Keywords: tsunami hazard maps; Cascadia Subduction Zone, tsunami risk, triangular dislocation model

1. Introduction

Large tsunamis destroy coastal communities and cause huge economic losses as well as large number of fatalities. Reliable tsunami hazard assessments play a crucial role to specify the at-risk coastal communities and predict the possible economic losses and provide warning and evacuation protocols. West coast of USA is vulnerable to the tsunami waves generated from Cascadia Subduction zone. Historical Cascadia earthquake on 1700 with a moment magnitude (Mw) of ~9 generated a mega tsunami that produced two fronts: one front hit the west coast of USA, and the other traveled across the Pacific Basin and caused damage along the Japanese coast. The earthquake and tsunami in 1700 are recorded in Native North American's imageries and stories [1] as well as radiocarbon dating, tree-ring dating studies, and Japanese written records [2], [3].

In terms of numerical modeling of tsunami waves at west of USA, Venturato et al., 2007 [4] modeled one tsunami scenario that was considered as the regeneration of 1700 Cascadia tsunami event and studied the tsunami propagation and inundation along the south-west Washington coast in Long Beach and Ocean Shores regions. González et al., 2009 [5] provided a set of tsunami events generated from Alaska-Aleutian, Kamchatka, Kuril, Southern Chile, and Cascadia subduction zone and studied their impacts on Seaside, Oregon region. Witter et al., 2011[6] studied the coastal inundation at Bandon Coos County in Oregon using 15 hypothetical scenarios in Alaska and Cascadia subduction zone. The above studies provided valuable information in terms of tsunami hazard assessment. However they mainly used a small number of possible tsunami scenarios for Cascadia subduction zone and their studies were mostly focused on a specific region.

To provide a comprehensive tsunami hazard assessment for entire west coast of USA including Washington, Oregon, and California coastlines, we developed a set of non-uniform slip distributions along the Cascadia subduction zone to predict the possible future tsunami generating earthquake events in this region. Then the fault surfaces are discretized using Delaunay triangles and a triangular dislocation model is used to model the seafloor/coastline uplift and subsidence due to the earthquake events using the fault geometry and non-uniform slip distributions. The cross sections of seafloor/coastline deformation profiles are presented at several important coastal cities. Then the seafloor/coastline deformations are given to a high-resolution numerical model to predict the tsunami wave propagations and corresponding coastal inundations. The tsunami hazard maps are developed for the entire west coast of USA and histograms of maximum wave height at key coastal cities as well as coastal inundation extends are provided. In addition, the historical 1700 Cascadia tsunami event is regenerated and the maximum wave heights offshore of USA west coastlines as well as coastal inundations are provided.

2. Tsunami dislocation model

When a mega earthquake occurs, the land as well as seafloor can experience large deformations including subsidence and uplifts. The offshore uplifts generate tsunami waves that propagate towards the coastlines. When we model the tsunami hazard generated from the near-field seismic sources, it is crucial to model the complex geometry of the fault surfaces accurately since the coastal subsidence and coastal inundations are very sensitive to the accuracy of the fault geometry and deformation pattern details. Displacements, strains, and stresses associated with faulting from earthquake ruptures can be calculated using elastic dislocation theory. Fault surfaces are often characterized by a set of points and rectangular sources and the deformations due to slip on rectangular sources are calculated using analytical solutions [7]. However some faults have complex geometries with fast variations in strike and dip and the rectangular sources are not capable of accurate presentation of the fault surface.

Therefore in this study the triangular dislocation model [8], [9], which presents a gap-free representation of fault surfaces using triangular meshes, is used to characterize the Cascadia Subduction faults. Meade (2007) [9] presented algorithms to analytically calculate the displacements on a triangular dislocation element by applying a dislocation loop where the deformation field for each of the triangle legs is calculated by superposition of two angular dislocations. More information on the analytical equations of displacement on a triangle element can be found in Meade (2007) [9].

To develop a comprehensive study on the tsunami hazard risk from Cascadia subduction zone, we model sets of non-uniform slip distributions along the CSZ for multiple geometries and moment magnitudes estimated from scaling relation. The non-uniform slip distributions are generated using the method by [10]. While we are using a comprehensive set of non-uniform slip distributions, we apply subjective criteria to remove none tsunami causing realizations of slip as well as physically unrealistic solutions of the stochastic method. The slip distributions are then constrained by the paleo-seismic records [11], [6] of offshore uplifts along west of USA and 259 unique tsunami generating earthquake events are selected to perform tsunami modeling. The geometries of the faults are discretized by Delaunay triangles and the triangular dislocation model is used to find the deformation patterns for each event. Fig 1 shows the west coast of USA with several vulnerable coastal cities to tsunami hazard. In this study, the west coast of USA is covered by 17 high resolution grids and the detailed seafloor/coastline deformation patterns due to 259 earthquake events are calculated. The resolution and the locations of high resolution grids will be discussed in more details in section 3.

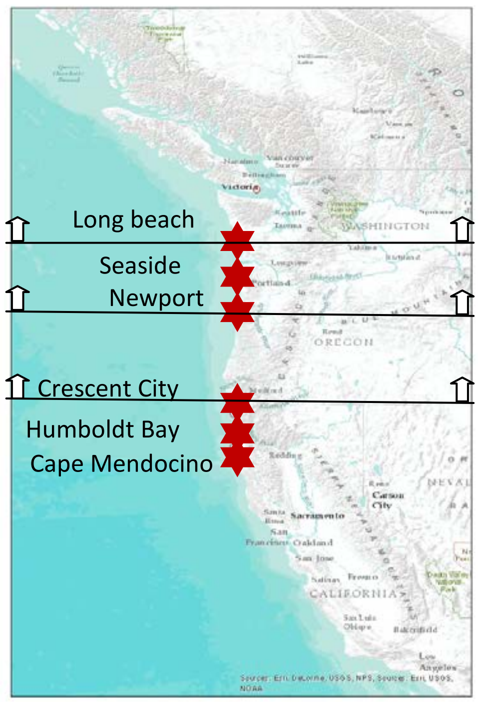

Fig 1: West Coast of USA vulnerable to tsunami hazard generated from the Cascadia subduction zone. The horizontal lines illustrate the cross sections that will be disscussed in fig 2

Fig 2 illustrates the cross sections of the initial deformations of seafloor and coastal land including uplift and subsidence at Long Beach, Washington, Newport, Oregon, and Crescent city, California corresponding to the set of earthquake events. This figure shows that the earthquake events are covering a wide range of offshore uplift from minimum of ~2m to maximum of ~15m that corresponds to a complete set of tsunami generating events.

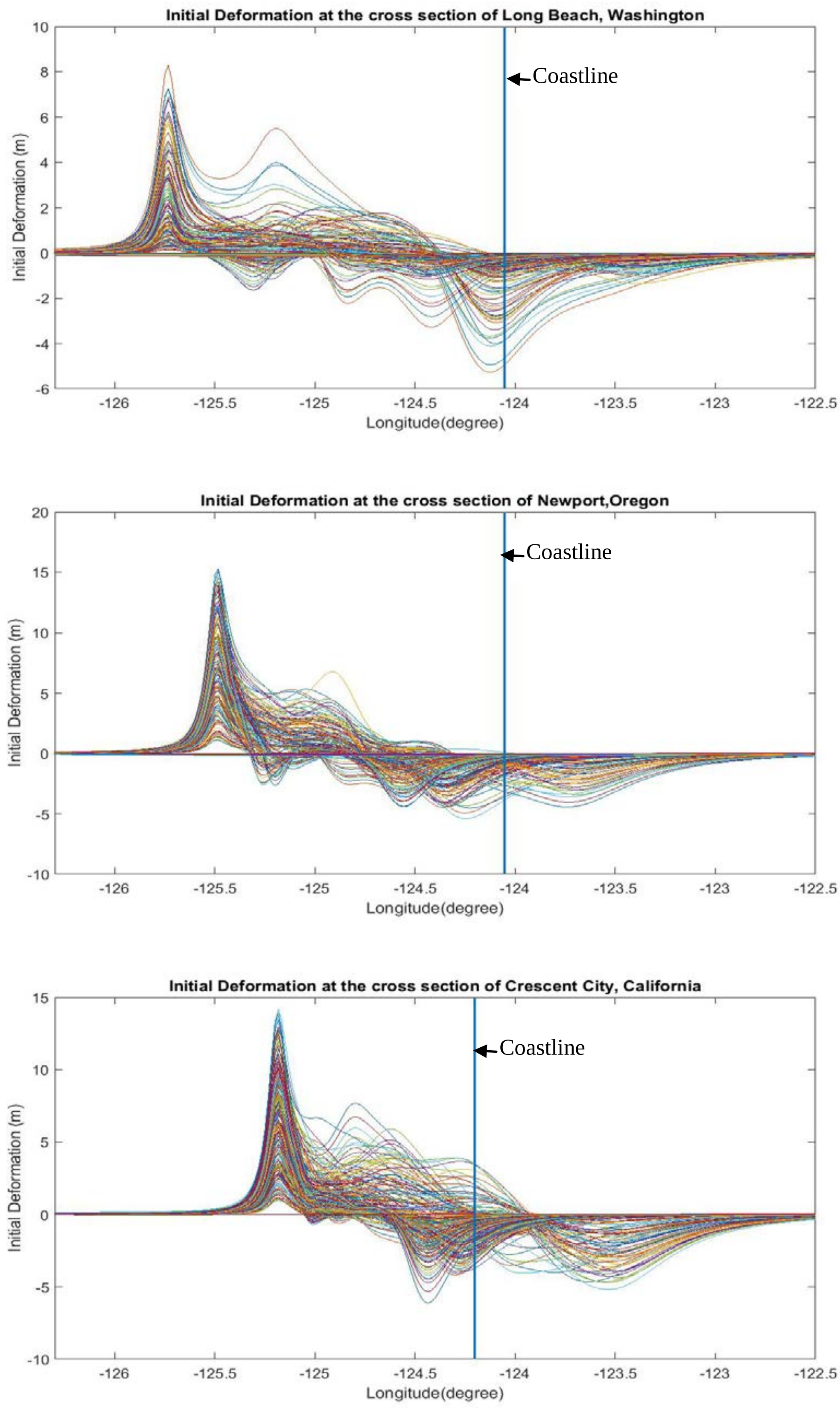

Fig 2. Initial deformations (uplift and subsidence) at cross sections of Long Beach, Washington, Newport, Oregon, and Cresent city, California corresponding to the earthquake set (The location of cross sections is shown in Fig. 1)

Coastlines of Long Beach, Newport, and Crescent city are experiencing a subsidence of maximum 5m. It is interesting to note that Crescent city coastline experiences uplift at some events due to fault geometry.

3. Tsunami wave model

3.1 Methodology

Tsunami wave modeling for this study is based on nonlinear shallow water equations that are numerically computed using the Finite Volume Method. To model the entire west coast of USA, three levels of imbedded grids with different resolutions are used to perform the numerical modeling. Fig 3 shows these three levels:

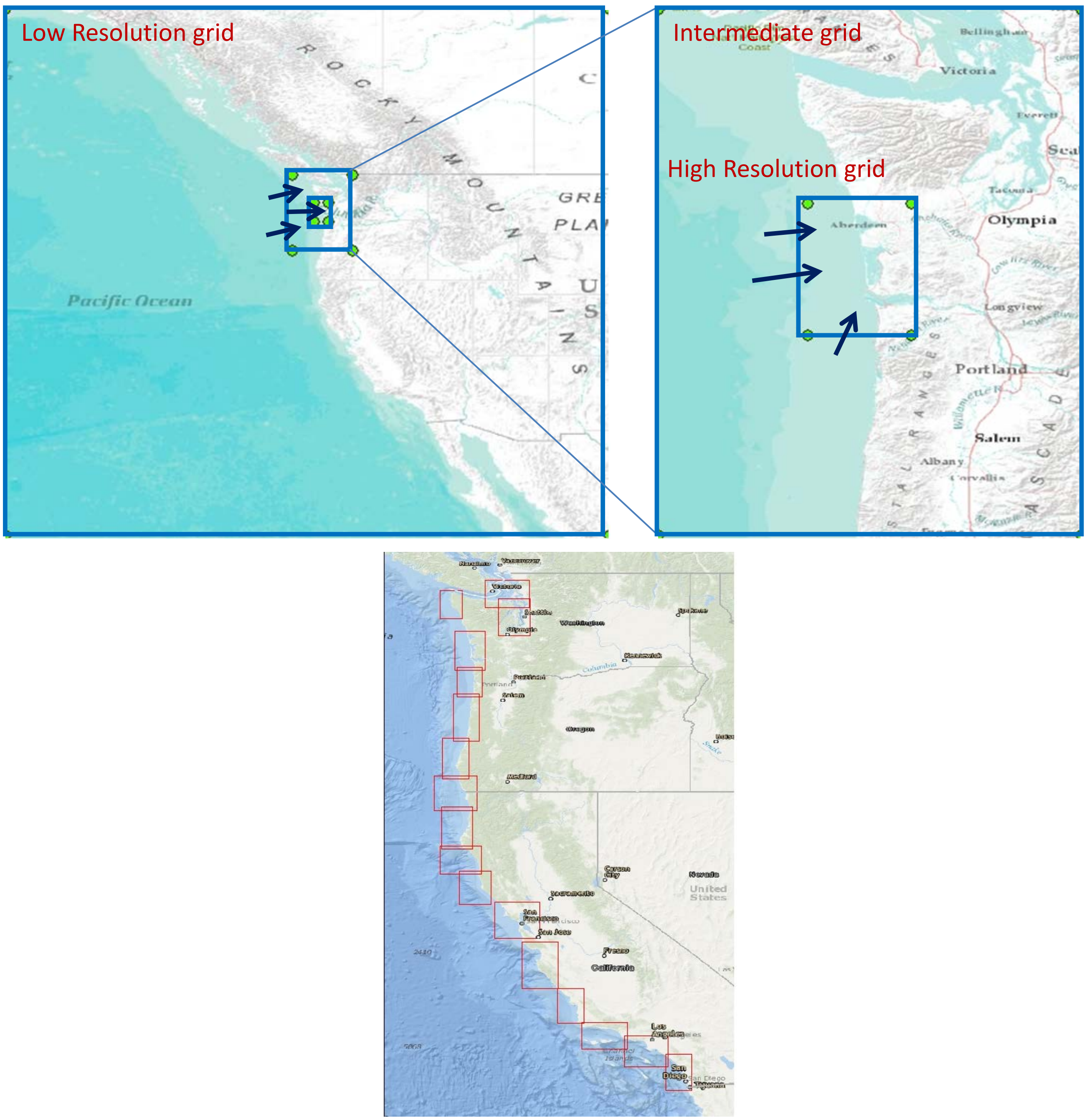

Fig 3. Computational grids: Top: A simple of three levels of embedded grids. Bottom: 17 High resolution grids covering west coast of USA

Pacific region Grid of relatively coarse (~1 km) resolution (Low resolution grid), 5 grids of intermediate (~100m) resolution (intermediate grid), and 17 grids of fine (~50m) resolution (High resolution grid). The pacific region grid (low resolution grid) of ~1 km grid is derived from GEBCO, 2014 gridded bathymetric data sets that include global terrain models for ocean and land [12]. 5 grids of intermediate (~ 100m) resolution and 17 grids of fine (~ 50m) resolution are resampled from NOAA bathymetric/topographic grids of ~90m and ~10m resolution covering the west coast of USA [13], [14], [15], [16], [17], [18], [19], [20], [21], [22], [23], [24]. The grids and the model output of wave elevations are referenced to mean sea level.

The bathymetric/topographic computational grids are adjusted in each 259 earthquake events to account for the seafloor/land deformation as explained in section 2. In each event, the vertical deformation values (including subsidence and uplift) are added to the bathymetric and topographic elevation values. The low resolution, intermediate, and high resolution grids interact with each other by passing boundary conditions between nodes along the intersecting boundaries. At the grids boundaries, wave heights as well as wave velocities in horizontal directions (x and y) are used as the boundary conditions. The low resolution grid passes data to the intermediate grids and the intermediate grids pass data to the high resolution grids. As the wave travels to shallower water, the resolution of grids become finer to accurately model the shorter wavelengths. For all the grids including Low resolution, intermediate and high resolution grids, both land and ocean is considered in the numerical simulations to take into account the complicated wave dynamics, refraction, diffraction, wave reflection, and other coastal processes.

The initial sea surface displacement at the time of tsunami generation (initial tsunami wave) is assumed to be identical to the seafloor/land deformation. To perform an accurate hydrodynamic modeling of wave run-up and coastal inundation, variable surface roughness is considered in the wave model. The existence of vegetation or man-made structures alerts the amount and pattern of tsunami inundation. Therefore it is important to consider the variable surface roughness based on the land cover data. For the west of USA, variable surface roughness is estimated using the Manning's coefficient derived from the land use data of high resolution National Land Cover Dataset (NLDC) by the US Geologic Survey (USGS) [25], [26]. To overcome the large computational efforts needed to apply the numerical wave modeling on the above grids for 259 earthquake events, parallel computing on Graphic Processing Units (GPUs) is implemented. The numerical model is run for 6 hours after the generation of the tsunami waves to model the full lifetime of tsunami waves and coastal processes.

3.1 Historical 1700 tsunami event

The 1700 Cascadia tsunami hit the west USA coastlines on January 26 at 0500 UTC with an estimated momentum magnitude of 8.7-9.2. Tsunami waves also traveled the Pacific Ocean and caused damage at Japanese coastlines. Several earthquake rupture models were proposed to estimate the slip distribution along the CSZ during the 1700 tsunami event using paleo-seismic evidences of coastal subsidence. Priest et al., 1997 [27] proposed six scenarios of slip distribution corresponding to the 1700 Cascadia tsunami event. Later Walsh et al., 2000 [28] modified one of the scenarios and added an asperity offshore of Washington State to take into account anomalies detected by satellite and seismic profiling.

In this study the slip distribution proposed in [28] is used to simulate 1700 Cascadia earthquake event. This slip distribution corresponds to an M_w 9.1 earthquake along CSZ. The average slip along fault is 17.5m and an asperity is added offshore of Washington State. The asperity location is centered at 47.324° N, 124.94° W and is generated using an elliptical Gaussian distribution. The asperity amplitude is equal to 4.5m and elliptical semi major axes are equal to 38.45 km and 25.63 km. The fault surface is discretized by Delaunay triangles and the initial deformation of seafloor and coastal land due to 1700 Cascadia earthquake is computed using the triangular dislocation model mentioned in section 2 and the slip distribution proposed in [28]. Fig.4 illustrates the offshore and onshore deformation (uplift and subsidence) due to 1700 Cascadia event from British Colombia, Canada coast in north to Oregon coast in south. The deformation in our study is compared with the seafloor/coastal land deformation reported in [4]. In both studies, the highest uplift is equal to 5-8m on west part of the subduction zone. Offshore of Washington state experiences uplift deformations of about 6m due to slip asperity in that location. Coastal land experiences subsidence of -3m to -1m. The slip distributions and the moment magnitudes (M_w = 9.1) are the same in our study and Venturato et al., 2007 [4] study. However the source geometries are slightly different, which result in different deformation values at some locations. For instance along the west corner of CSZ, the uplift values in our study are higher than the values reported in [4].

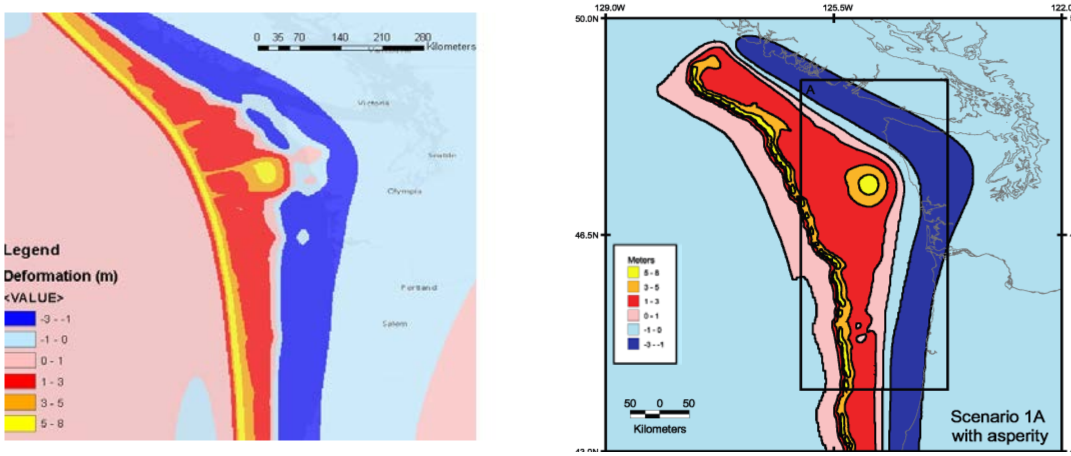

Fig 4. Left: Initial deformation of seafloor and coastal land associated with 1700 Cascadia earthquake event using slip distribution of [29]. Right: Initial deformation reported in [4]

The numerical model is used to model the tsunami wave propagation and coastal inundations. To model the worst case scenario, the state of the tide is set as Mean High tide (MHW).The maximum wave amplitudes at different stations offshore of Oyhut, Ocean shores, Ocean Park, Oceanside, and Seaview in Washington State are compared to previous studies ([4],[28]) and presented in fig 5. The pattern of maximum wave amplitudes in our study is similar to [4]. However the wave values are higher in our study. The reason is that the initial offshore uplift (initial tsunami wave) is higher in our study in comparison to initial uplift in [4] (see the uplift values at the west corner of rupture in Fig. 4). In addition, we have used an updated data of high resolution bathymetric and topographic data. To further validate our numerical results of 1700 historical tsunami event, the numerical inundation in Seaside Oregon is compared to the locations of observed tsunami deposits [29], [30]. Fig. 6 shows the numerical results as well as the observed tsunami deposits corresponding to 1700 tsunami event. The tsunami deposits were found in the locations that were not developed or otherwise disturbed since 1700. Therefore they show the minimum inundation areas. As illustrated in fig. 6, our numerical results have reached and inundated the locations of tsunami deposit observations.

3.2 Cascadia tsunami events

We developed a set of non-uniform slip distributions along the CSZ corresponding to large moment magnitude events of higher than 8.0 that are capable of generating tsunami events. The slip distributions are then constrained by the paleo-seismic records [11], [6] of offshore uplifts along west of USA and 259 unique tsunami generating earthquake events are selected. The fault geometries are discretized by Delaunay triangles and the triangular dislocation model is used (as discussed in section 2) to calculate uplift and subsidence offshore and onshore of west USA coastlines for each earthquake event.

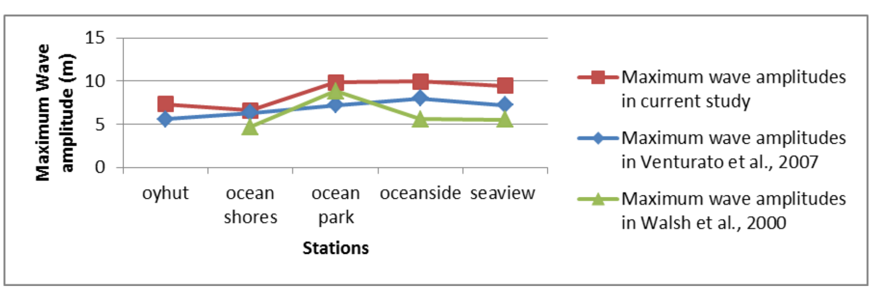

Fig 5. Maximum wave amplitude at different stations offshore of Washington state

Non-uniform pattern of slip distributions presents a more realistic presentation of the earthquake events whereas the uniform slip distributions are much more simplified and are not able to provide a comprehensive understanding of tsunami hazards. Variable slip distribution leads to a variety of possible initial tsunami wave characteristics including variable wave heights and variable wavelengths that have a direct impact on the intensity and extends of coastal inundations. Since non-uniform slip models are used, some events have higher offshore uplift (initial tsunami wave) at northern part and have higher impact on Washington state coastlines and lower impact on north California coastlines. On the other hand, some events have higher offshore uplift (initial tsunami wave) at southern part of subduction zone and have higher impacts on Oregon coastlines and north California coastlines.

The numerical wave model is used by the aid of GPU parallel computation to model the tsunami wave propagation and coastal inundation for each event along the entire west coast of USA. As discussed in section 3.1, three levels of imbedded computational grids (with different resolutions) are used to accurately model the wave propagation as well as coastal processes including wave reflection, refraction, diffraction and finally the coastal inundation. The tsunami hazard maps including the inundation depths and tsunami extends are developed. Fig. 6 presents the histograms of maximum wave heights at several coastal cities including Cape Mendocino, Humboldt Bay, and Crescent city in California, Newport in Oregon, Seaside and Long Beach in Washington. It is notable that Cape Mendocino and Humboldt Bay cities are pretty close to each other but tsunami impact on Humboldt Bay is higher than Cape Mendocino. The reason is related to the coastline curvature at that region. The tsunami waves partially reflect back as they hit the curvature. Fig 7 shows a sample of coastal inundation in Long Beach, Washington and Crescent city, California. The earthquake events, corresponding to the tsunami inundations shown in this figure, generated the highest initial uplift (initial tsunami wave peak) at the cross section of Long beach and Crescent city and therefore the largest tsunami extends are anticipated. The largest coastal inundations can be correlated to the height of initial uplift at some regions but other parameters such as bathymetry and topography profiles, characteristics of land cover, coastal phenomena such as secondary waves, and reflective waves play an important role in the extends of tsunami inundations.

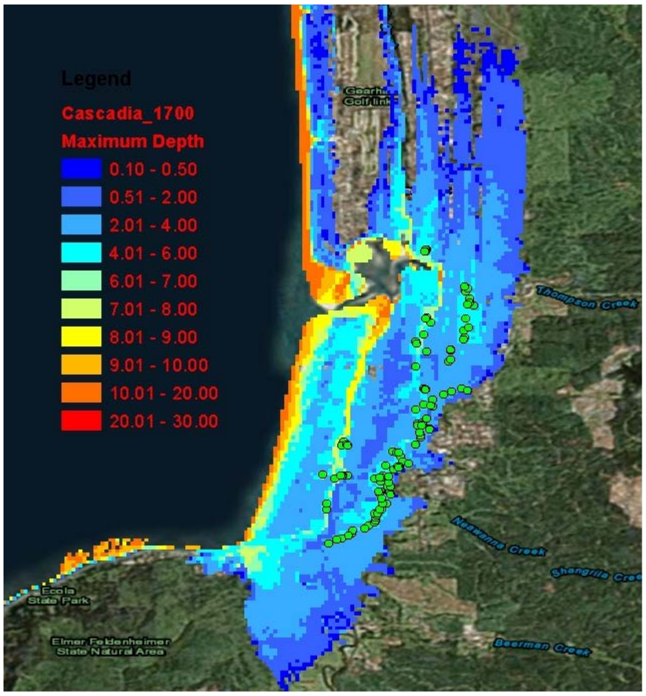

Fig 6. Numerical results of histrorical 1700 tsunami inundation and the locations of the tsunami deposits in Seaside region (The Green circles shows the locations of tsunami deposits[29], [30])

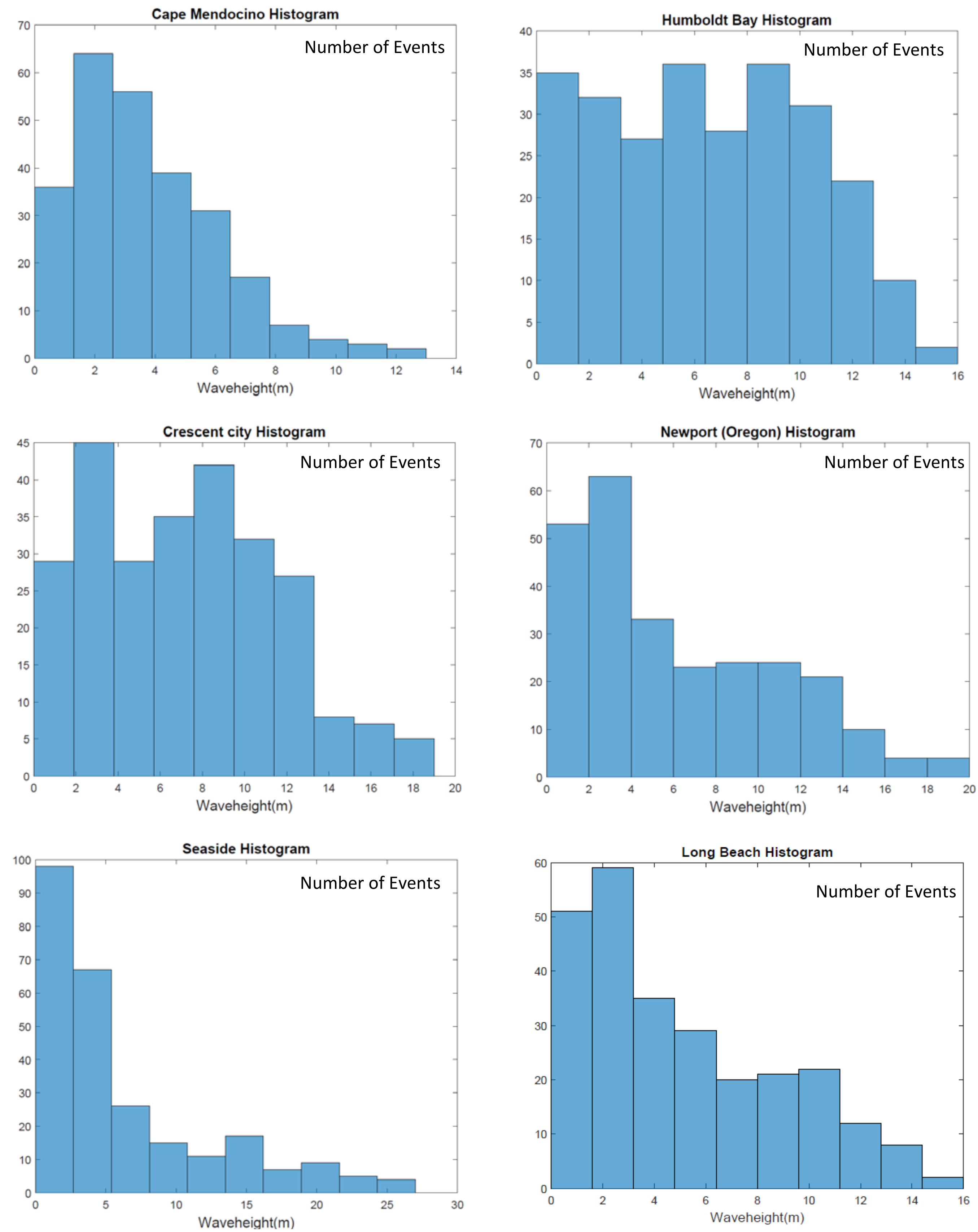

Fig 7. Histogram of maximum wave heights at coastal cities along West coast of USA (Total number of events = 259)

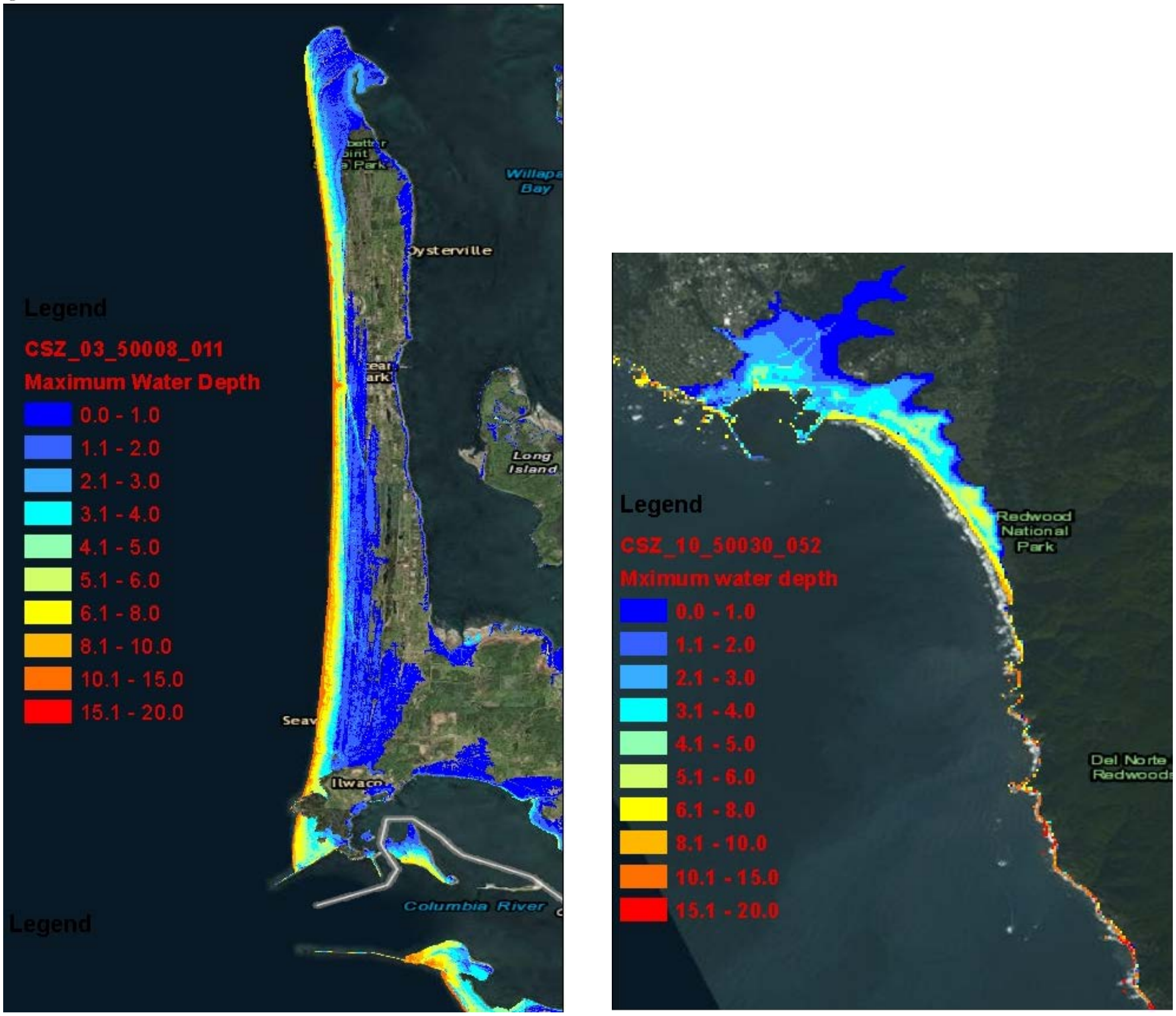

Fig 8. Sample of Tsunami inundation extends for two tsunami events. Left: Long Beach, Washington, Right: Crescent City, California

4. Conclusions and Future works

We developed tsunami hazard maps corresponding to a wide range of possible earthquake events in Cascadia subduction zone along the west coast of USA including Washington, Oregon, and California coastlines on high resolution bathymetric and topographic grids. Non-uniform slip distributions are used to present realistic tsunami generating seismic events and an advanced triangular dislocation model is implemented to capture the complexity of fault geometries and provide gap-free deformation fields including uplift and subsidence offshore and onshore of USA coastlines. We implemented hydrodynamic modeling using three levels of imbedded computational grids to model wave propagation, wave reflection, refraction, diffraction and the maximum coastal inundation along USA west coastlines. Variable land roughness based on the land cover classes is used to accurately model the tsunami run-up and maximum inundation extends. This paper covers the tsunami hazard assessment for west coast of USA due to Cascadia Subduction Zone. In parallel RMS has performed an extensive development on tsunami vulnerability model, utilizing state-of-the-art empirical analysis techniques (Charvet et al., 2014, 2015 [31], [32]) on detailed tsunami damage data, combined with a novel analytical engineering-based approach. This method allows for a bespoke estimation of tsunami vulnerability for the US West coast. In addition, a detailed exposure model for the west coast of the USA has been developed. In future we will take into account the frequency of tsunami generating earthquake events and combine the hazard model with the vulnerability model and exposure model to achieve a comprehensive tsunami risk assessment for coastal cities on west of USA and improve the risk management due to large tsunamis.

5. Acknowledgements

We are grateful to Kelly Carignan for her useful comments and helpful communications to use NOAA bathymetric and topographic data sets. We also thank M. Mai for useful input and availability of source modeling software.

6. References

[1] Ludwin R. S., Dennis R., Carver D., McMillan A. D., Losey R., Clague J., Jonientz-Trisler Ch., Bowechop J., Wray J., James K (2005): Dating the 1700 Cascadia Earthquake: Great Coastal Earthquakes in Native Stories, *Seismological Research Letters*,**62** (2), 140-148.

[2] Satake K., Shimazaki K., Tsuji Y., and Ueda K. (1996): Time and size of a great earthquake in Cascadia inferred from Japanese tsunami records of January1700. *Nature*, **379** (6562), 246–249.

[3] Yamaguchi D.K., Atwater B.F., Bunker D.E., Benson B.E., and Reid M.S. (1997): Tree-ring dating in the 1700 Cascadia earthquake. *Nature*, **389** (6654), 922– 924.

[4] Venturato A.J., Arcas D., Kânoğlu U., (2007) Modeling Tsunami Inundation from a Cascadia Subduction Zone Earthquake For Long Beach and Ocean Shores, Washington, *NOAA Technical Memorandum OAR PMEL-137*

[5] González F.I., Geist E.L., Jaffe B., Kânoğlu U., Mofjeld H., Synolakis C. E.,Titov V. V., Arcas D., Bellomo D., Carlton D., Horning T., Johnson J., Newman J., Parsons T., Peters R., Peterson,G. Priest C., Venturato A., Weber J., Wong F., Yalciner A. (2009) Probabilistic tsunami hazard assessment at Seaside, Oregon, for near- and far-field seismic sources, *Journal of Geophysical Research*, **114** (C11023), 1-19

[6] Witter R. C., Zhang Y., Wang K., Priest G. R., Goldfinger Ch., Stimely L.L., English J.T, Ferro P.A. (2011) Simulating Tsunami Inundation at Bandon, Coos County, Oregon, Using Hypothetical Cascadia and Alaska Earthquake Scenarios, *Oregon Department of Geology and Industries special paper*, ORS 516.030.

[7] Okada, Y. (1985) Surface deformation due to shear and tensile faults in a half-space. *Bulletin of the Seismological Society of America* **75**, 1135–1154.

[8] Yoffe E.H. (1960) The angular dislocation, *Phil. Mag.* **5**, 161-175.

[9] Meade B. J. (2007) Algorithms for the calculation of exact displacements, strains, and stresses for triangular dislocation elements in a uniform elastic half space, *Computers & Geoscience* 1064-1075.

[10] Mai P.M., Beroza G.C. (2002) A spatial random field model to characterize complexity in earthquake slip, *J Geophys Res*,**107**, 1-21.

[11] Goldfinger, C., Nelson, C.H., Morey, A.E., Johnson, J.E., Patton, J.R., Karabanov, E., Gutiérrez-Pastor, J., Eriksson, A.T., Gràcia, E., Dunhill, G., Enkin, R.J., Dallimore, A., and Vallier, T. (2012) Turbidite event history—Methods and implications for Holocene paleoseismicity of the Cascadia subduction zone, *U.S. Geological Survey Professional Paper* 1661–F, 170 p. (Available at http://pubs.usgs.gov/pp/pp1661f/).

[12] Sandwell,D.T., Gille,S.T., and Smith, W.H.F., eds. (2002) Bathymetry from Space:Oceanography, Geophysics, and Climate, Geoscience Professional Services, Bethesda, Maryland.

[13] Friday D.Z., Taylor L.A., Eakins B.W., Warnken R.R., Carignan K.S., Caldwell R.J., Lim E., Grothe P.R (2010) Digital Elevation Model of Arena Cove, California: Procedures, Data Sources and Analysis, *NOAA Technical Memorandum NESDIS NGDC-39.*

[14] Love M.R., Friday D.Z., Grothe P.R, Carignan K.S., Eakins B.W., Taylor L.A (2012) Digital Elevation Model of Astoria, *NOAA Technical report*.

[15] Carignan K.S., Taylor L.A., Eakins B.W., Warnken R.R., Lim E., Grothe P.R (2009) Digital Elevation Model of Central Oregon Coast: Procedures, Data Sources and Analysis, *NOAA Technical Memorandum NESDIS NGDC-25.*

[16] Grothe P.R, Taylor L.A., Eakins B.W., Carignan K.S., Caldwell R.J., Lim E., Friday D.Z. (2011) Digital Elevation Model of Crescent City, California: Procedures, Data Sources and Analysis, *NOAA Technical Memorandum NESDIS NGDC-51*.

[17] Sutherland M.G., Taylor L.A, Love M.R., Eakins B.W., Carignan K.S. (2013) Digital Elevation Model of Garibaldi, Oregon, *NOAA Technical report*.

[18] Taylor L.A., Eakins B.W., Carignan K.S, Warnken R.R., Sazonova T., Schoolcraft D. C. (2008) Digital Elevation Model of La Push, Washington : Procedures, Data Sources and Analysis, *NOAA Technical Memorandum NESDIS NGDC-14.*

[19] Grothe P. R., Taylor L.A., Eakins B.W., Carignan K.S, Friday D.Z., Love M.R. (2012) Digital Elevation Model of Monterey, California : Procedures, Data Sources and Analysis, *NOAA Technical report*.

[20] Carignan K.S., McLean S.J., Eakins B.W., Beasley L., Love M.R., Sutherland M. (2014) Digital Elevation Model of Puget Sound, Washington: Procedures, Data Sources and Analysis, *NOAA Technical report*.

[21] Carignan K.S., Taylor L.A., Eakins B.W., Friday D.Z., Grothe P. R., Love M.R., (2012) Digital Elevation Model of San Diego, California: Procedures, Data Sources and Analysis, *NOAA Technical report*.

[22] Carignan K.S., Taylor L.A., Eakins B.W., Caldwell R. J., Friday D.Z., Grothe P. R., Lim E. (2011) Digital Elevation Model of Central California and San Francisco Bay : Procedures, Data Sources and Analysis, *NOAA Technical Memorandum NESDIS NGDC-52.*

[23] Carignan K.S., Taylor L.A., Eakins B.W., Warnken R.R., Lim E., Medley P. R. (2009) Digital Elevation Model of Santa Barbara California: Procedures, Data Sources and Analysis, *NOAA Technical Memorandum NESDIS NGDC-29.*

[24] Grothe P. R., Taylor L.A., Eakins B.W., Carignan K.S., Warnken R.R., Lim E., Caldwell R. J. (2010) Digital Elevation Model of Taholah, Washington: Procedures, Data Sources and Analysis, *NOAA Technical Memorandum NESDIS NGDC-34.*

[25] Kalyanapu A. J., Burian S. J., McPherson T. N. (2009) Effect of land use-based surface roughness on hydrologic model output, *Journal of Spatial Hydrology*, **9(2)**, 51-71.

[26] Homer, C.G., Dewitz, J.A., Yang, L., Jin, S., Danielson, P., Xian, G., Coulston, J., Herold, N.D., Wickham, J.D., and Megown, K.(2015) Completion of the 2011 National Land Cover Database for the conterminous United States-Representing a decade of land cover change information, *Photogrammetric Engineering and Remote Sensing*, **81(5)**, 345-354.

[27] Priest, G.R., Myers III E.P., Baptista A.M., Fleuck P., Wang K., Kamphaus, R.A., Peterson C.D. (1997) Cascadia subduction zone tsunamis—Hazard mapping at Yaquina Bay, Oregon, *Oregon Department of Geology and Mineral Industries*, Open-File Report O-97-34, 144 pp.

[28] Walsh, T.J., Caruthers C.G., Heinitz A.C., Myers III E.P., Baptista A.M., Erdakos G.B., Kamphaus R.A. (2000) Tsunami hazard map of the southern Washington Coast: Modeled tsunami inundation from a Cascadia subduction zone earthquake, *Washington Division of Geology and Earth Resources Geologic Map*, **49**, 3-12.

[29] Fiedorowicz, B.K., Peterson, C.D. (2002) Tsunami deposit mapping at Seaside,Oregon, USA, in Bobrowski, P.T., ed., Geoenvironmental mapping: methods,theory, and practice: Lisse, The Netherlands, A. A. Balkema Publishers, 629-648.

[30] Wong, F.L., Venturato, A.J., Geist, E. L. (2006) Seaside, Oregon Tsunami Pilot Study -- Modernization of FEMA Flood Hazard Maps: GIS Data: U.S. Geological Survey Data Series 236, U.S. Geological Survey, Menlo Park, California.

[31] Charvet, I., Suppasri, A., Kimura, H., Sugawara, D. & Imamura, F. (2015) A multivariate generalized linear tsunami fragility model for Kesennuma City based on maximum flow depths, velocities and debris impact, with evaluation of predictive accuracy. *Natural Hazards*, **79 (3)**, 2073-2099

[32] Charvet, I., Ioannou, I., Rossetto, T., Suppasri, A., & Imamura, F. (2014) Empirical fragility assessment of buildings affected by the 2011 Great East Japan tsunami using improved statistical models. *Natural Hazards*, **73(2)** 951-973.